Osteoarthritis and Cartilage 27 (2019) 304–313

Osteoarthritis and Cartilage

Raman spectroscopy-based water content is a negative predictor of articular human cartilage mechanical function

M. Unal † ‡ §, O. Akkus ‡ § ‖ ¶ *, J. Sun #, L. Cai ††, U.L. Erol ‡, L. Sabri ‡, C.P. Neu †† ‡‡

† Department of Mechanical Engineering, Karamanoğlu Mehmetbey University, Karaman 70100, Turkey
‡ Department of Mechanical and Aerospace Engineering, Case Western Reserve University, Cleveland, OH 44106, USA
§ Center for Applied Raman Spectroscopy, Case Western Reserve University, Cleveland, OH 44106, USA
‖ Department of Orthopaedics, Case Western Reserve University, Cleveland, OH 44106, USA
¶ Department of Biomedical Engineering, Case Western Reserve University, Cleveland, OH 44106, USA
# Department of Population and Quantitative Health Sciences, Case Western Reserve University, Cleveland, OH 44106, USA
†† Weldon School of Biomedical Engineering, Purdue University, West Lafayette, IN 47907, USA
‡‡ Department of Mechanical Engineering, University of Colorado Boulder, Boulder, CO 80309, USA

ARTICLE INFO

Article history:
Received 14 February 2018
Accepted 8 October 2018

Keywords:
Water
Osteoarthritis
Raman spectroscopy
Permeability
Aggregate modulus
Magnetic resonance imaging

SUMMARY

Objective: Probing the change in water content is an emerging approach to assess early diagnosis of osteoarthritis (OA). We herein developed a new method to assess hydration status of cartilage nondestructively using Raman spectroscopy (RS), and showed association of Raman-based water and organic content measurement with mechanical properties of cartilage. We further compared Raman-based water measurement to gravimetric and magnetic resonance imaging (MRI)-based water measurement.

Design: Eighteen cadaveric human articular cartilage plugs from 6 donors were evenly divided into two age groups: young ($n = 9$, mean age: 29.3 ± 6.6) and old ($n = 9$, mean age: 64.0 ± 1.5). Water content in cartilage was measured using RS, gravimetric, and MRI-based techniques. Using confined compression creep test, permeability and aggregate modulus were calculated. Regression analyses were performed among RS parameters, MRI parameter, permeability, aggregate modulus and gravimetrically measured water content.

Results: Regardless of the method used to calculate water content (gravimetric, RS and MRI), older cartilage group consistently had higher water content compared to younger group. There was a stronger association between gravimetric and RS-based water measurement ($R_g^2 = 0.912$) than between gravimetric and MRI-based water measurement ($R_c^2 = 0.530$). Gravimetric and RS-based water contents were significantly correlated with permeability and aggregate modulus whereas MRI-based water measurement was not.

Conclusion: RS allows for quantification of different water compartments in cartilage nondestructively, and estimation of up to 82% of the variation observed in the permeability and aggregate modulus of articular cartilage. RS has the potential to be used clinically to monitor cartilage quality noninvasively or minimally invasively with Raman probe during arthroscopy procedures.

Published by Elsevier Ltd on behalf of Osteoarthritis Research Society International.

Introduction

Detecting the early stage of osteoarthritis (OA) is crucial to decelerate or reverse the progression of OA by enabling interventions such as weight-loss and life style changes[1]. However, identification of an early onset OA marker that can be measured noninvasively and/or nondestructively has been elusive to date.

A potential candidate for early diagnosis of OA is cartilage hydration. In the canine model of early OA generated by transection of the anterior cruciate ligament (ACL), increased water content in the superficial zone was observed as early as 3 weeks after the operation despite the fact that histological changes were minimal[2,3]. Increased water content up to 10–15% was also found in osteoarthritic human cartilage compared to healthy group[4–6]. The

* Address correspondence and reprint requests to: O. Akkus, Department of Mechanical and Aerospace Engineering, Case Western Reserve University, 10900 Euclid Ave, Cleveland, OH 44106, USA. Tel: 1-216-368-4175.
E-mail addresses: mustafa.unal@case.edu (M. Unal), ozan.akkus@case.edu (O. Akkus).

https://doi.org/10.1016/j.joca.2018.10.003
1063-4584/Published by Elsevier Ltd on behalf of Osteoarthritis Research Society International.

permeability of water within the highly negatively charged extracellular matrix is critical to physiological and mechanical functions of cartilage[7] such as transportation of nutrients to chondrocytes, lubrication of cartilage surface[8], and load bearing capacity of cartilage[9]. Therefore, water is an ideal biomarker of assessing early diagnosis of OA. Measurement of water content may provide information on the status of cartilage quality and early diagnosis of OA; however, methods are limited for non-invasive and non-destructive measurement of cartilage water content. The standard gravimetric measurement requires excision and dehydration of tissue; therefore, it is not applicable clinically. To date, magnetic resonance imaging (MRI) is the only non-destructive technique to assess hydration status of cartilage[10–12], but its execution is not without limitations. Detecting small changes in water content of cartilage is challenging with MRI because of limited spatial resolution and the partial-volume averaging effects[13,14].

Raman spectroscopy (RS) may be an ideal method to assess hydration status of cartilage. RS has been predominantly used to study collagen and proteoglycan (PG) phases in the fingerprint region of cartilage spectrum (800–1800 cm^{-1})[15,16]. A comprehensive analysis of cartilage water is possible through the analysis of higher wavenumber region of the spectrum between 2700 and 3800 cm^{-1}. Standard RS systems have limited sensitivity in studying hydration range because of reduced quantum efficiency of charged coupled detectors (CCDs) in this region. Recently, we built a short-wave infrared (SWIR) RS system with sensitivity maximized in the 2700+ cm^{-1} range to assess different water fractions in bone[17–20]. Using this SWIR RS, we have recently investigated OH stretch band of bovine articular cartilage, and identified contributions of bound and unbound water fractions in the OH-stretch band[21].

To the best of our knowledge, water content of healthy and diseased human cartilage has not been measured by RS previously. Furthermore, there has not been any attempt to study associations between Raman-based cartilage biomarkers and specific mechanical properties (e.g., aggregate modulus and permeability). Finally, there has not been any validation of MRI-based water content measures by secondary and tertiary methods. The current study quantified Raman spectra, MRI relaxometry and mechanical properties of cartilage from healthy young and older distal femoral cartilage to shed light on these issues. Confirmation of Raman-based water content's associations with cartilage mechanics in controlled specimens is essential prior to non-invasive execution of Raman using recently emerging techniques such as spatially offset RS[22] or Raman tomography[23].

Materials and methods

Cartilage specimen preparation

Full-thickness (~2 mm; 4 mm diameter) cylindrical cartilage plugs were harvested from primary load-bearing portions of lateral femoral condyle (LFC) and medial femoral condyle (MFC), and patellofemoral groove (PFG)[24] (n = 18) of six fresh-frozen human femurs with no known diseases (male, 21–65 years-old; Musculoskeletal Transplant Foundation, Edison, NJ, USA). Cartilage plugs were evenly divided into two age groups: young (n = 9, 29.3 ± 6.6, age 21 to 36) and old (n = 9, 64.0 ± 1.5, ages 62 to 65). Specimens were kept hydrated at all times in 1× phosphate buffered saline (PBS) except when they were stored at −20 °C. Prior to measurements, specimens were thawed for at least 2 h in PBS at room temperature.

Gravimetric water measurement

The excess PBS on specimen surface was gently blotted and wet weight of specimens was measured three times (Model XS64, Mettler-Toledo, Columbus, OH), and change in weight was found to be within 1–2%. Change in wet weight before and after Raman data collection was within 0.6%, indicating water loss is limited during RS measurement. Following Raman analysis, specimens were dried in an oven at 37°C for 48 h and weighed again for dry weight. This temperature and duration time effectively removed unbound (mobile) water to steady state as shown by 95% reduction in OH-band intensity[21].

The percent water was calculated as:

$$\text{Water \% by weight} = 100 \times (W_w - W_d)/W_w \quad (1)$$

where W_w was the initial wet weight of cartilage and W_d was the weight after oven drying.

SWIR RS data collection and processing

A customized SWIR RS-system was used in this study[17,18]. The system (Supplemental Fig. 1) used a 847 nm (Axcel Photonics) laser source, and a shortwave InGaAs IR spectrometer (BaySpec, Inc., CA, USA) specifically optimized for 1000–1400 nm wavenumber range that corresponded to the spectral range of ~2550–4770 cm^{-1}, which covered the CH and OH-stretch bands.

Articular surface was chosen for RS measurement since it is the first region to exhibit morphological and biochemical alterations with the early hallmark of OA[25,26]. All Raman spectra were obtained at the articular surface from 3 equidistant points to cover the region of interest. Each spectrum was obtained as the average of 10 consecutive spectra with each collected for 10 s. Laser power was set to ~25 mW on the specimen to avoid possible water loss and matrix damage associated with excessive laser heating[27].

Spectra collected from three locations per specimen were averaged firstly. Then, using piecewise linear segments, the background was removed from the spectra by subtracting the fitted fluorescence baseline, and spectra were further smoothed to improve signal-to-noise ratio using a de-noising algorithm (LabSpec 5, Horiba Scientific, Edison, NJ). The spectra were then fitted through second derivative analysis to identify peak locations. Intensity ratios (I_{OH}/I_{CH}) at the following wavenumbers were calculated: ~3200/2940, ~3250/2940, ~3450/2940, ~3520/2940, and ~3650/2940. ~3250/2940, and ~3450/2940 ratios represent collagen-related water molecules while ~3520/2940 represents PG-related water molecules. ~3650/2940 represents both collagen- and PG-related water molecules as identified in our previous publication[21]. The intensity ratio of ~3450/3250 was calculated as an indicator of water bonding states in cartilage[21]. The area under the OH band (A_{OH}) was calculated as an estimate of total water content and the area under CH-stretch band (A_{CH}) was calculated as a measure of organic content. The ratio of areas (A_{OH}/A_{CH}) was calculated as a measure of water per unit organic content.

Biomechanical testing

Mechanical measurements were carried out in a confined compression creep setting using a custom-made instrument as shown in Supplemental Fig. 2. A dead-weight generating 19 kPa compressive stress 'σ' was applied on the specimen and creep displacement of the plunger was recorded until equilibrium (within 10,000 s). Stress was calculated from the applied load and cartilage cross-sectional area. Strain was calculated from the initial thickness and creep displacement. Aggregate modulus H_A was calculated by using the following equation[28].

$$\frac{u(t)}{h} = \frac{\tilde{P}_A}{H_A}\left(1 - \frac{2}{\pi^2}\sum_{n=0}^{\infty}\frac{\exp\left(-\left(n+\frac{1}{2}\right)^2\pi^2 H_A k t/h^2\right)}{\left(n+\frac{1}{2}\right)^2}\right) \quad (2)$$

where u represents the displacement vector; h, cartilage thickness:$\tilde{P}_A$, constant compression load; H_A, aggregate modulus and k, permeability.

Permeability k was estimated by fitting the experimental creep curve to the zeroth order analytical solution of the one dimensional confined compression creep equation as follows[7].

$$k = -4{*}h^2\frac{\log(\pi^2(1-\varepsilon(t)/(8H_A/\sigma)}{(\pi^2 H_A t)} \quad (3)$$

where $\varepsilon(t)$ is the strain at time t.

MRI data collection and processing

Morphology images were first acquired (7T, Bruker Medical GmbH, Ettlington, Germany) using a 3D (i.e., 2D multislice) Rapid Acquisition with Refocused Echoes (RARE) sequence. Following image parameters were used: echo time (TE)/repetition time (TR) = 31.82/3000 ms; number of echoes = 8; number of averages = 4; in-plane resolution = 0.098 × 0.098 mm^2; matrix size = 256 × 256 pixels^2; and slice thickness = 1.0 mm; number of slices = 3. In a single image slice defined from the center of the volume image, we acquired spatial (pixel-by-pixel) maps of T_2 relaxation times, i.e., common metrics used to assess cartilage structure and health[10]. T_2 imaging parameters were: TE = [7.95, 15.91, 23.86, 31.82, 39.77, 47.73, 55.68, 63.64] ms; TR = 3000 ms; number of averages = 2; number of echo images = 8. T_2 relaxation times were determined at each pixel using a two parameter exponential curve-fitting algorithm in MATLAB (Mathworks, Natick, MA).

Statistical analysis

All statistical analyses were performed using Minitab 17 statistical software (State College, PA) or R (rproject.org). Some variables appeared to follow a normal distribution and some do not (e.g., Permeability, $Area_{OH}/Area_{CH}$, and 3 sub-bands ratios) based on our exploratory data analysis (EDA). No outliers were detected by Grubbs and Dixon's test. Due to the sample size and clustering of plugs within donors the test from modeling by General Estimating Equation (GEE) (suitable for clustering of plugs in subjects and without normality assumption) were performed to test a possible difference between young and old groups, in all variables (Table I). Linear regressions were performed among Raman variables, MRI variables, aggregate modulus and gravimetrically measured water content. Regression analyses were conducted using GEE and mixed effects (LMM) models, which accounted for the clustering of plugs in subjects and where the GEE models are also not limited by the normality assumption. The regression analysis models included age (young vs old as a binary variable), predictor variable (mechanical property etc.) and the interaction between the two terms. The following R-squared values are calculated: 1) generalized R-square value[29] for GEE analysis (R^2_g), 2) marginal R-square and conditional R-square (Refs.[30,31] for LMM analysis (R^2_m and R^2_c). In the Results section and in Figure legends, we provide the best of the three R-squared values for the sake of brevity whereas Table II lists all R-squared values for further reference. Several relationships involving 'permeability' displayed apparently nonlinear exponential growth/decay relationships for which logarithmic transformation was performed to linearize the data prior to LMM/GEE analyses. All the R-squares provided in the study were associated with the model that had P-values for the predictor of interest (either by itself or via its interaction with the age in binary format) as $P < 0.05$, though some are much more significant than the others in consistency with those shown in R-squares. Statistical significance was considered at P-value <0.05.

Results

Differences between Raman data of the two age groups

Raman measures for organic content as reflected by CH_2 intensity ($P = 0.0003$), [Fig. 1(a) and Table I] and area under CH_2 (Fig. 2, $P = 0.0001$) were greater for young age group. Area of the main OH peak (~3450–3500 cm^{-1}) differed between the two age groups ($P = 0.035$, Table I). OH-intensities normalized by CH_2 intensities (the amount of water per organic content) were greater for older specimens than that of younger specimens [Fig. 1(b)]. Second derivative analysis showed five peaks for young (3200, 3250, 3442, 3520, and 3630 cm^{-1}) and old cartilage (3200, 3250, 3451, 3531, and 3650 cm^{-1}) [Fig. 1(c)].

Raman, gravimetric and MRI-based hydration properties

Gravimetric, Raman ($Area_{OH}$ and $Area_{OH}/Area_{CH}$) and MRI-based water contents of old cartilage was greater than that of young

Table I
Mean ± St. Dev values for mechanical properties, gravimetric, Raman, and MRI-based hydration parameters of the two age groups. N.S. = not significant according to GEE based comparison

Property	Young ($n = 9$)	Old ($n = 9$)	P-value GEE
Permeability (m^4/N s)	1.67 ± 2.48 × 10^{-13}	1.69 ± 1.77 × 10^{-13}	N.S.
Aggregate modulus (MPa)	0.21 ± 0.08	0.11 ± 0.07	**3.1e-08**
Gravimetric water (% by weight)	75.37 ± 1.83	79.32 ± 2.20	**2.6e-06**
T_2 (ms)	36.48 ± 7.86	45.40 ± 8.01	**0.00038**
$Area_{OH}/Area_{CH}$	6.67 ± 0.50	7.47 ± 0.94	**0.019**
$Area_{OH}$	9331 ± 754	9869 ± 712	**0.035**
$Area_{CH}$	1508 ± 110	1332 ± 127	**0.00011**
$Intensity_{CH}$	92.40 ± 11.40	79.46 ± 7.59	**0.00033**
$Intensity_{OH}$	148.43 ± 9.86	143.51 ± 8.27	N.S.
I_{3200}/I_{2940}	1.15 ± 0.22	1.32 ± 0.26	**0.0055**
I_{3250}/I_{2940}	1.45 ± 0.15	1.47 ± 0.13	N.S.
I_{3450}/I_{2940}	1.61 ± 0.24	1.94 ± 0.26	**0.00095**
I_{3520}/I_{2940}	1.27 ± 0.21	1.52 ± 0.24	**6.5e-05**
I_{3650}/I_{2940}	0.56 ± 0.06	0.64 ± 0.15	N.S.
I_{3450}/I_{3250}	1.30 ± 0.04	1.34 ± 0.02	**0.011**

Significant p-values (< 0.05) are in bold

Table II
R-square values that obtained from marginal LMM, conditional LMM and GEE-based regression analysis. Marginal and conditional LMM associated R-squares are denoted as R^2_m, R^2_c, respectively, and generalized R-square is denoted as R^2_g for GEE. The gray highlighted tabulated R-square values refer the best of the three models for the given variable

Property	Linear regression	Non-linear regression (Exponential growth/decay)	GEE	LMM R^2_m = m: marginal fixed effects	LMM R^2_c = c: conditional fixed and random factors
Gravimetric water vs $Area_{OH}/Area_{CH}$	$R^2 = 0.79$	_	$R^2_g = 0.912$	$R^2_m = 0.886$	$R^2_c = 0.908$
Gravimetric water vs T_2 (ms)	$R^2 = 0.30$	_	$R^2_g = 0.630$	$R^2_m = 0.630$	$R^2_c = 0.530$
T_2 (ms) vs $Area_{OH}/Area_{CH}$	$R^2 = 0.31$	_	$R^2_g = 0.437$	$R^2_m = 0.401$	$R^2_c = 0.756$
T_2 (ms) vs $Area_{OH}$	$R^2 = 0.29$	_	$R^2_g = 0.427$	$R^2_m = 0.361$	$R^2_c = 0.596$
Gravimetric water vs Aggregate modulus (MPa)	$R^2 = 0.51$	_	$R^2_g = 0.652$	$R^2_m = 0.618$	$R^2_c = 0.748$
$Area_{OH}/Area_{CH}$ vs Aggregate modulus (MPa)	$R^2 = 0.45$	_	$R^2_g = 0.536$	$R^2_m = 0.495$	$R^2_c = 0.679$
$Area_{OH}$ (a.u.) vs Aggregate modulus (MPa)	$R^2 = 0.17$	_	$R^2_g = 0.240$	$R^2_m = 0.182$	$R^2_c = 0.199$
$Area_{CH}$ (a.u.) vs Aggregate modulus (MPa)	$R^2 = 0.44$	_	$R^2_g = 0.649$	$R^2_m = 0.599$	$R^2_c = 0.748$
$Intensity_{CH}$ (a.u.) vs Aggregate modulus (MPa)	$R^2 = 0.50$	_	$R^2_g = 0.566$	$R^2_m = 0.535$	$R^2_c = 0.627$
Gravimetric water vs Permeability (m^4/N s)	_	$R^2 = 0.44$	$R^2_g = 0.874$	$R^2_m = 0.813$	$R^2_c = 0.891$
$Area_{OH}/Area_{CH}$ vs Permeability (m^4/N s)	_	$R^2 = 0.51$	$R^2_g = 0.844$	$R^2_m = 0.620$	$R^2_c = 0.817$
$Area_{OH}$ (a.u.) vs Permeability (m^4/N s)	_	$R^2 = 0.47$	$R^2_g = 0.534$	$R^2_m = 0.534$	$R^2_c = 0.666$
$Area_{CH}$ (a.u.) vs Permeability (m^4/N s)	_	$R^2 = 0.40$	$R^2_g = 0.787$	$R^2_m = 0.733$	$R^2_c = 0.733$
$Intensity_{CH}$ (a.u.) vs Permeability (m^4/N s)	_	$R^2 = 0.37$	$R^2_g = 0.622$	$R^2_m = 0.559$	$R^2_c = 0.769$
I_{3200}/I_{2940} vs Aggregate modulus (MPa)	$R^2 = 0.42$	_	$R^2_g = 0.553$	$R^2_m = 0.615$	$R^2_c = 0.829$
I_{3250}/I_{2940} vs Aggregate modulus (MPa)	$R^2 = 0.41$	_	$R^2_g = 0.267$	$R^2_m = 0.231$	$R^2_c = 0.231$
I_{3450}/I_{2940} vs Aggregate modulus (MPa)	$R^2 = 0.42$	_	$R^2_g = 0.584$	$R^2_m = 0.560$	$R^2_c = 0.739$
I_{3520}/I_{2940} vs Aggregate modulus (MPa)	$R^2 = 0.53$	_	$R^2_g = 0.643$	$R^2_m = 0.614$	$R^2_c = 0.681$
I_{3650}/I_{2940} vs Aggregate modulus (MPa)	$R^2 = 0.45$	_	$R^2_g = 0.570$	$R^2_m = 0.512$	$R^2_c = 0.679$
I_{3450}/I_{3250} vs Aggregate modulus (MPa)	$R^2 = 0.44$	_	$R^2_g = 0.455$	$R^2_m = 0.408$	$R^2_c = 0.408$
I_{3200}/I_{2940} vs Permeability (m^4/N s)	_	$R^2 = 0.39$	$R^2_g = 0.433$	$R^2_m = 0.409$	$R^2_c = 0.513$
I_{3250}/I_{2940} vs Permeability (m^4/N s)	_	$R^2 = 0.37$	$R^2_g = 0.396$	$R^2_m = 0.404$	$R^2_c = 0.570$
I_{3450}/I_{2940} vs Permeability (m^4/N s)	_	$R^2 = 0.34$	$R^2_g = 0.571$	$R^2_m = 0.532$	$R^2_c = 0.599$
I_{3520}/I_{2940} vs Permeability (m^4/N s)	_	$R^2 = 0.38$	$R^2_g = 0.548$	$R^2_m = 0.520$	$R^2_c = 0.634$
I_{3650}/I_{2940} vs Permeability (m^4/N s)	_	$R^2 = 0.37$	$R^2_g = 0.403$	$R^2_m = 0.362$	$R^2_c = 0.758$
I_{3450}/I_{3250} vs Permeability (m^4/N s)	_	$R^2 = 0.29$	$R^2_g = 0.423$	$R^2_m = 0.451$	$R^2_c = 0.841$

cartilage ($P < 0.0001$, $P = 0.019$, $P = 0.035$, $P = 0.00038$, respectively) (Fig. 2 and Table I). The association between gravimetric and Raman based water content was highly significant ($R^2_g = 0.912$) [Fig. 3(a)]. MRI-based hydration measure was also significantly correlated with gravimetric water content ($R^2_g = 0.630$) (mostly within the old group based on GEE analyses) and Raman based hydration measure ($R^2_c = 0.756$ and $R^2_c = 0.596$) [Fig. 3(b)–(d)] (in older group). Among sub-bands intensities normalized by CH_2 intensity, all ratios except 3250/2940 and 3650/2940 significantly differed between the groups (Table I).

Mechanical property variation between groups

Aggregate modulus of older specimens was significantly lower than that of young specimens ($P < 0.0001$) [Fig. 4(a) and Table I] whereas permeability did not differ between the two groups ($P > 0.05$) [Fig. 4(b) and Table I].

Associations of Raman parameters with permeability

The associations between water content and permeability were nonlinear when two groups were merged together (i.e., ignore the group effect) and appear so in some subgroup cases (Fig. 5). Permeability increased with increasing gravimetric water content [$R^2_c = 0.891$ (group and clustering effects considered), Fig. 5(a)], Raman-based water content per unit organic content [$R^2_g = 0.844$, Fig. 5(b)] (more significant for the old group) and with increasing amount of Raman-based non-normalized OH band area [$R^2_c = 0.666$, Fig. 5(c)]. MRI-based hydration was not correlated significantly to permeability ($P > 0.10$).

Permeability was negatively and nonlinearly associated with organic content such that permeability decreased with increasing organic content initially, then it reached a steady state [$R^2_g = 0.787$ and $R^2_c = 0.769$, respectively, Fig. 5(d) and (e)].

All five sub-bands ratios were nonlinearly associated with permeability [$R^2_c = 0.570$–0.758, Sup. Fig. 3(a)–(e) and Table II]. The trends of the relationships of sub-bands were comparable to the trend that was observed for the entire OH-band [Fig. 5(b) and (c) and Table II]. ~3450/3200 ratio was nonlinearly related to permeability [$R^2_c = 0.841$, Sup. Fig. 3(f) and Table II].

Associations of Raman parameters with aggregate modulus

Specimens with greater water content had lower aggregate modulus, both for gravimetric [$R^2_c = 0.748$, Fig. 6(a) and Table II] and Raman-based water content measures [$R^2_c = 0.680$, Fig. 6(b) and Table II]. Normalization of water content by protein content enhanced the strength of the association ($R^2_c = 0.680$ vs $R^2_g = 0.240$) [Fig. 6(b) vs 6(c) and Table II]. Specimens with greater Raman intensities for organic phase had greater aggregate modulus ($R^2_c = 0.748$ and $R^2_c = 0.627$), [Fig. 6(d) and (e) and Table II]. MRI-based water content was not significantly associated with aggregate modulus ($P > 0.10$).

The sub-bands intensities were negatively associated with the aggregate modulus [$R^2_c = 0.231$, ..., 0.829, Sup. Fig. 4(a)–(e) and Table II]. Normalized band intensities at ~3200 and ~3520 cm^{-1} had

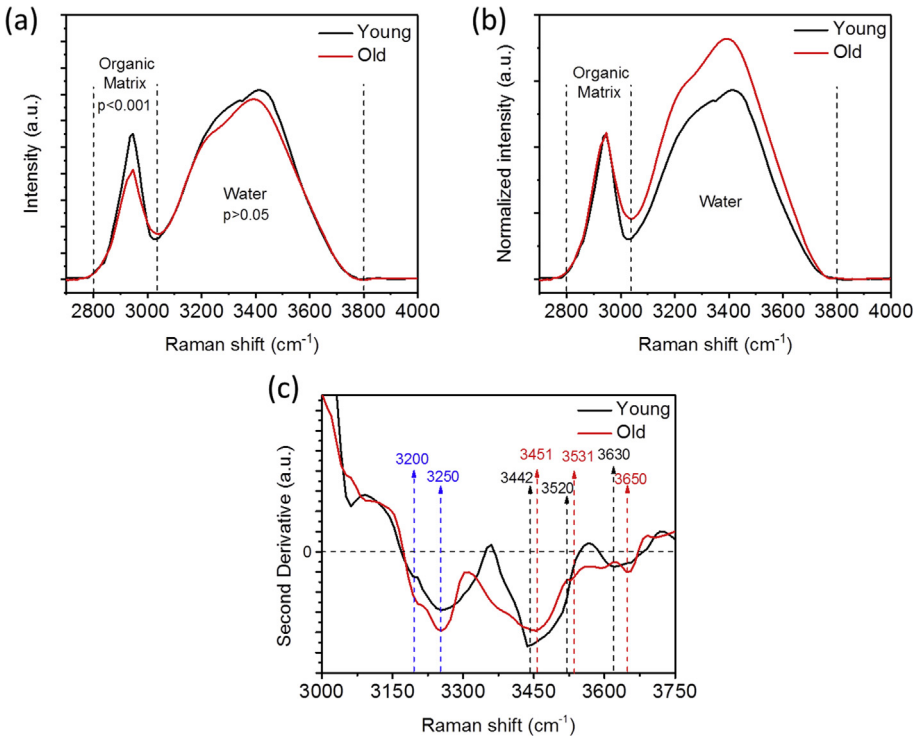

Fig. 1. (a) Raman spectra of younger and older age groups obtained by averaging twenty-seven spectra collected at three different locations from nine cartilage specimens per group from both groups. The standard deviation was within %12 of the intensity and not shown in the spectra for the sake of clarity. The wavenumber range of 2700–3050 cm^{-1} manifests CH_2-stretch band associated with organic (i.e., collagen and PG phases of cartilage) matrix whereas OH-stretch band extends across 3050–3800 cm^{-1}. Greater amount of organic matrix is reflected by Raman intensities. (b) Raman spectra obtained after normalizing the spectra to match organic matrix intensity indicates that older specimens had greater water amount per organic content. (c) Second derivative analysis revealed the locations of sub-bands making up the water region for the two groups. Bands for older specimens appeared at greater wavenumbers than those of younger specimens.

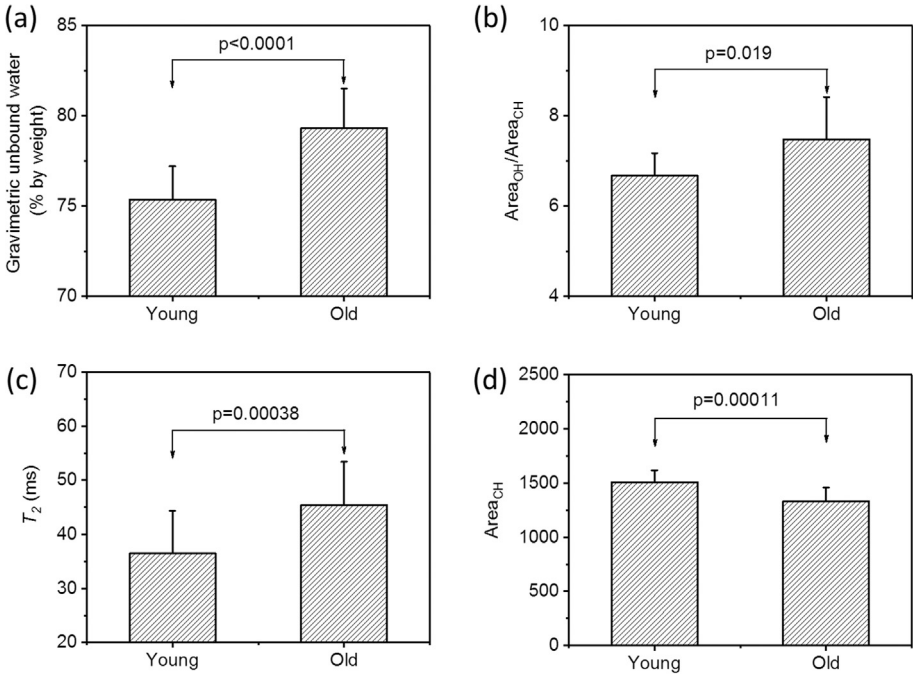

Fig. 2. Older cartilage group consistently has higher water content compared to younger group, regardless of the method used to calculate water content: (a) gravimetric, (b) RS and (c) MRI. (d) Organic matrix content as an area under CH_2–band was significantly greater in young cartilage specimens compared to old cartilage specimens.

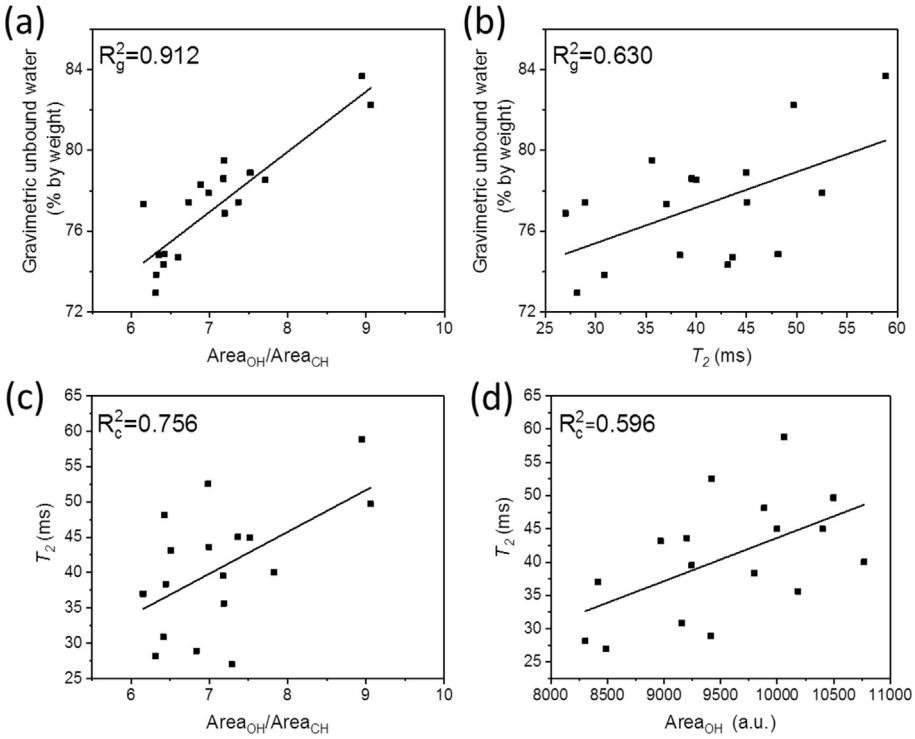

Fig. 3. Associations between (a) gravimetric and Raman-based ($Area_{OH}/Area_{CH}$), (b) gravimetric and MRI-based (T_2), and (d) MRI (T_2) and Raman ($Area_{OH}$)-based measures of hydration.

the highest association with aggregate modulus [R_c^2 = 0.829 and 0.739, respectively, Sup. Fig. 4(d) and Table II].

Discussion

We demonstrated, for the first time, that Raman-based water measures have significant associations with aggregate modulus and hydraulic permeability of human articular cartilage. Raman-based water content was closely validated by gravimetric water content. Therefore, Raman-based water measurement is as effective as direct measurement of water content by gravimetric measurement [Fig. 2(a) vs 2(b)]. This is an important outcome because gravimetric measurement requires physical removal of water whereas RS analysis provides water content information from the native tissue without the need for dehydration. Therefore, Raman-based hydration may be a suitable biomarker to estimate mechanical function of cartilage.

MRI is the only nondestructive and clinically applicable method for measurement of water content. To the best of our knowledge, this is the first study that validated MRI-based hydration with secondary methods of Raman and gravimetric measurement, and, sought for associations between MRI measures and cartilage specific mechanical properties. An important finding of this study was that MRI-based T_2 relaxation time, as a surrogate for cartilage water content[32], was correlated to gravimetric [Fig. 3(b)] and Raman [Fig. 3(c) and (d)]-based hydration measures. Furthermore, MRI was able to resolve the differences between water contents of the young and old age groups [Fig. 2(c) and Table I]. On the other hand, although significant, the association of MRI-based water measure to gravimetric standard was lower than the association of RS-based water measure [Fig. 3(b) and Table II], and the need to improve the MRI detection sensitivity of cartilage damage in small sample sizes has been noted[10]. Future advancement of MRI acquisition and processing methods to improve hydration-based noninvasive predictor of cartilage quality may benefit from comparison to gravimetric and Raman measures as standards.

In agreement with earlier studies[33–38], our gravimetric and more importantly Raman-based water measurement showed

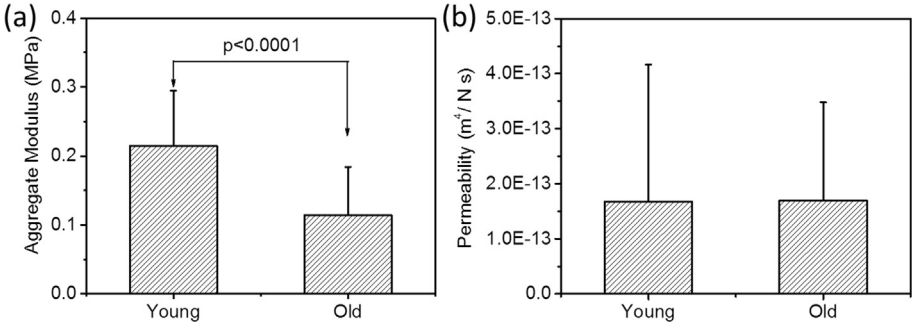

Fig. 4. Mean and standard deviation representations of (a) aggregate modulus and (b) permeability of the cartilage specimens from the two age groups.

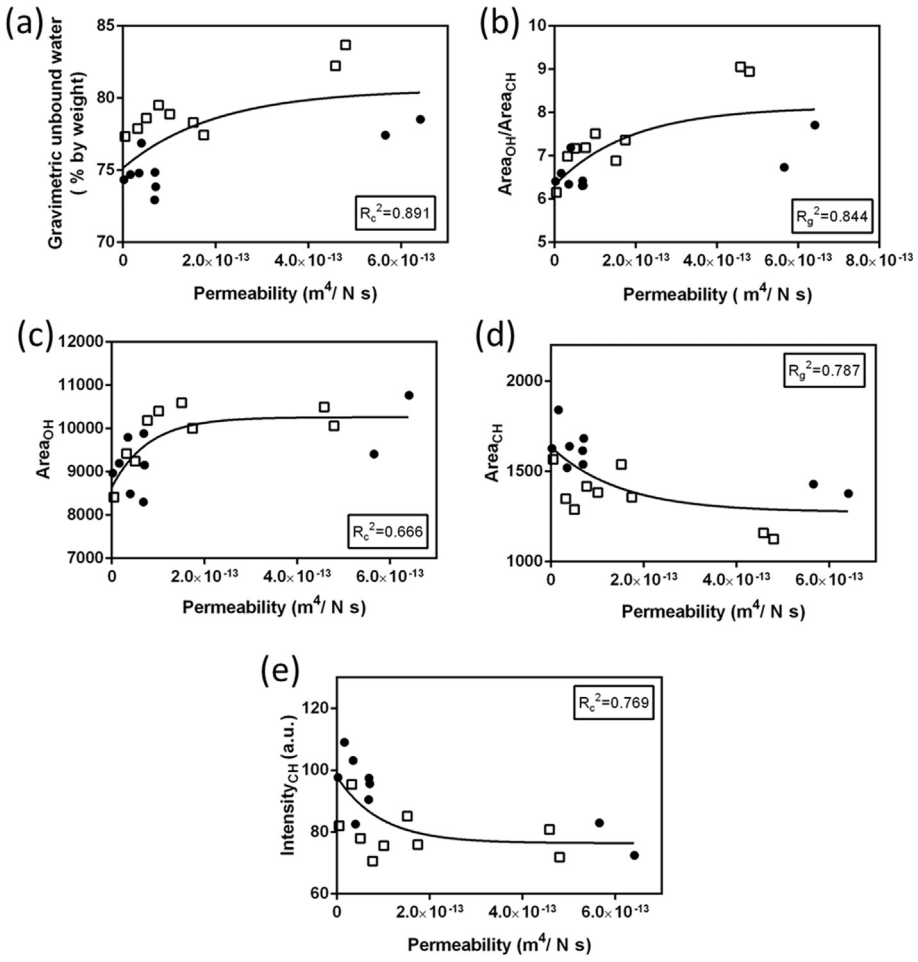

Fig. 5. Associations between permeability vs (a) gravimetric-, (b–c) Raman-based hydration measures and (d–e) Raman-based organic content. Open square indicates old cartilage group and black circle indicates young cartilage group. Reported R^2 values in the figures are the best model among conditional LMM R-square (R^2_c), marginal LMM R-square (R^2_m), or GEE-based R-square (R^2_g).

similar significant associations between water content and biphasic properties of human articular cartilage [Figs. 5 and 6, Sup. Figs. 3 and 4 and Table II]. Our results are also in good agreement with earlier studies[34–37,39] that used destructive techniques to measure organic matrix content. Raman-based organic matrix amount (based on measure of intensity or area of CH_2 peak nondestructively) is associated negatively with permeability [Fig. 5(d) and (e)] and positively with aggregate modulus [Fig. 6(d) and (e)], suggesting RS offers a non-destructive surrogate measurement of organic matrix content in cartilage. However, it is important to note that CH_2 peak is not specific to GAG or collagen, rather it emerges from both collagen and PGs.

A low permeability is mechanically desirable by rendering resistance to deformation of cartilage through limiting the flow of water[9,38]. While the permeability of cartilage specimens from old and young donors did not differ [Fig. 4(b) and Table I] likely due to high data scatter, significant nonlinear associations between permeability and water content emerged when data were pooled over donors (Fig. 5 and Sup. Fig. 3). We previously reported that ~95% of intensity within OH-stretch band is associated with unbound (free) water[21]. Therefore, it is plausible for the permeability to increase with more unbound (free) water. Organic phase in cartilage, particularly aggrecan, is known to attract and stabilize water molecules[40]. Therefore, one would expect lower water mobility, thus, lower permeability for cartilage tissue with greater organic content. This notion was supported by earlier studies[39,40] as well as by our data such that samples with high CH_2 band intensities or areas which are reflecting of the organic content had lower permeability values [Fig. 5(d) and (e)].

Aggregate modulus is a cartilage specific measure of organic matrix stiffness that is obtained from the latent stages of long-term mechanical testing at which effects of water on mechanical performance subsides. As expected, cartilage tissues with greater organic matrix contents were stiffer [Fig. 6(d) and (e)]. Furthermore, specimens with greater water content, which is an indicator of greater pore space, had lower aggregate modulus [Fig. 6(a)–(c) and Sup. Fig. 4(a)–(f)]. Therefore, water content is an indirect measure of cartilage stiffness by reflecting the pore volume within which the unbound water freely moves[9,38].

Recently, we reported that only ~ 4–5% of Raman signal is associated with bound water[21]. Given that analyzing bound water Raman signal in intact cartilage requires dehydration that is not clinically viable, we did not seek for associations between bound water and cartilage mechanical properties. As we identified in our previous study[21], different sub-bands in the OH-stretch band are associated with water molecules interacted with different organic matrix components in cartilage such as chondroitin sulfate or collagen[21]. The strengths of associations of permeability and

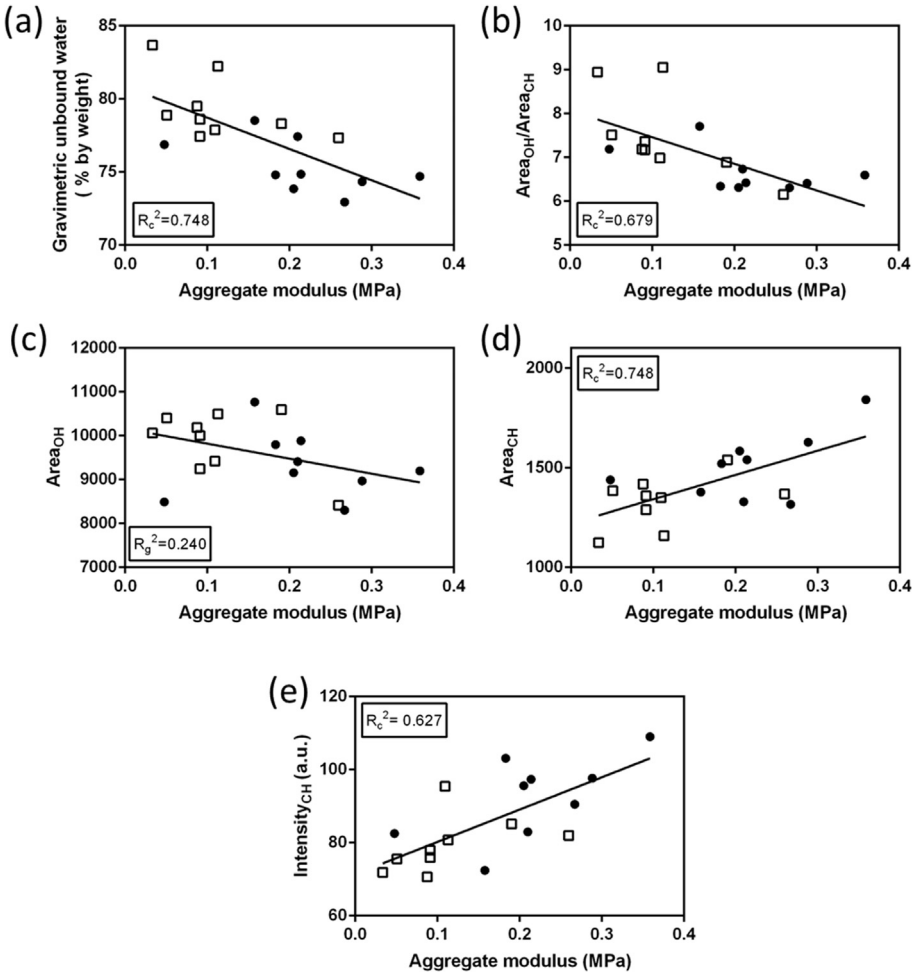

Fig. 6. Associations between aggregate modulus vs (a) gravimetric-, (b–c) Raman-based hydration measures and (d–e) Raman-based organic content. Open square indicates old cartilage group and black circle indicates young cartilage group. Reported R^2 values in the figures are the best model among conditional LMM R-square (R_c^2), marginal LMM R-square (R_m^2), or GEE-based R-square (R_g^2).

aggregate modulus with individual sub-band intensities (Figs. 3–6) were mostly weaker than those obtained by the entire OH band range. This outcome suggests that each water compartment contributes to cartilage mechanics, and that integrating the entire OH region to capture such discrete contributions improves the strength of association between permeability and water content.

We previously reported that ~3450/3250 is an indicator of water bonding states in cartilage[21]. The higher value indicates the decreased number of hydrogen bonds between water molecules and cartilage macromolecules (collagen and PGs), thereby, indicating of more free water in cartilage[21]. In this study, old cartilage group had higher value for this ratio compared to young cartilage group (Table I) and higher values of this ratio correlated with higher permeability [Sup. Fig. 3(f) and Table II] and lower aggregate modulus [Sup. Fig. 4(f) and Table II]. Thus, it can be used to assess association between water bonding states and cartilage quality.

Our findings suggest that the way water chemically interacts with its environment is different between young and old cartilage specimens, as indicated by differences in wavenumber locations of sub-bands [Fig. 1(c)]. For example, the peaks located between 3400 and 3700 cm^{-1} in the young group shifted to higher wavelength for old cartilage group [Fig. 1(c)]. Previously, we showed that the peaks located at lower wavenumber (~3200 and 3250 cm^{-1}) are related to water molecules with stronger hydrogen bonds while the peaks located at higher wavenumber (~3450 and ~3520 cm^{-1}) have weaker hydrogen bonds, and the peaks at the region of ~3630–3650 are non-hydrogen bond water molecules[21]. Thus, shifts to higher wavenumber indicate that there is more free and weaker hydrogen bonded water molecules in the specimens of the older cartilage. This finding agrees with previous reports of PG loss and collagen degradation with aging[38,39,41] and such diminishment in the organic phase results in reduction of water binding capacity of older cartilage.

Human cartilage water content has been measured in the past using gravimetric or MRI techniques with contradictory results reported[38,42–45] that may be attributed to age, location (patellar vs femoral head), and tissue source (cadavers vs joint replacement patients). On the other hand, past literature has consistently shown OA samples to have greater water content than healthy cartilage[4–6,46], as we observed for the sample set in this study [Fig. 2(a)–(c)]. Our specimens were collected from load bearing regions; therefore, it is more likely that the older group was at a higher state of degeneration than the younger group.

Near Infrared (NIR) spectroscopy is another emerging method to assess hydration status of cartilage[47,48]. Although NIR spectroscopy offers a superior penetration depth (~0.5–5 mm) in cartilage compared to RS (couple hundred μm), NIR spectrum bands are chemically less-specific and relatively harder to interpret. Mid-infrared (MIR) and fingerprint region of Raman spectrum have been widely used to assess the OA-associated biochemical changes in collagen and PGs[16,49]. Raman fingerprint region has been also

used recently to study depth-dependent water distribution[50] through the analysis of inherently weak water peak located at Amide I region. This water peak overlaps with prominent collagen and PG-related peaks. As confirmed[50], the higher wavenumber region is more suitable to analyze cartilage water. Taking all into consideration, vibrational spectroscopic techniques (Raman, NIR, and MIR) provide complementary information to evaluate biochemical changes in cartilage composition. Therefore, the combination of these techniques holds a great potential for a versatile assessment of cartilage matrix.

As a limitation, we collected Raman spectra from the articular surface. Although, robust associations between gravimetric water content that is resulting from bulk of cartilage and Raman-based water measurements from surface suggests that articular surface content to mirror the water content in the rest of cartilage. Early onset of cartilage degeneration is more pronounced on the mechanical loaded articular layer[25,26]; therefore, measurements conducted on this layer would be valuable. Because gravimetric and MRI-based water measurements provide the water content of entire cartilage volume, future RS studies are also needed to characterize the depth of penetration of the laser to cartilage to better define the sampling volume.

In conclusion, this study demonstrated that RS was able to explain ~90% of the variation in gravimetric water content, and was also able to resolve age-related changes in water content that corresponded to 5% of total cartilage wet weight as determined by gravimetric water content. Ability of RS to detect water content was also functionally meaningful such that up to 82% of the variation in aggregate modulus and permeability of cartilage could be explained by water content of cartilage as measured by RS. Given that gravimetric analysis cannot be conducted nondestructively, and also it cannot be executed in a site specific way, RS can become one of the few nondestructive tools to assess water content in cartilage. RS-based water measurement may be used as a biomarker of OA progression in animal model studies investigating drugs' efficacy or rehabilitation in longitudinal studies. In clinical practice, RS has the potential to measure water content in cartilage *in vivo* nondestructively and transcutaneously using emerging methods, i.e., spatially-offset RS[22] or fiber optic Raman probes during arthroscopic evaluation[15]. Visual arthroscopic evaluation is highly subjective to assess cartilage degeneration, and RS may supplement visual evaluation with matrix biochemistry and water content. Moreover, RS analysis may serve to benchmark MRI data in clinical studies.

Contributions

MU, OA and CPN conceived the study design. MU, LC and ULE performed the experiments. Data were analyzed by all authors. JS carried out the statistical analysis of data and wrote the segments of the manuscript associated with statistical methods. MU and OA primarily wrote the manuscript with contributions from the co-authors. All authors agree to the content of this manuscript.

Disclosures

All authors declare no conflict of interest.

Acknowledgments

This work was partially supported by think [box] at CWRU.

Supplementary data

Supplementary data to this article can be found online at https://doi.org/10.1016/j.joca.2018.10.003.

References

1. Gersing A, Solka M, Joseph G, Schwaiger B, Heilmeier U, Feuerriegel G, *et al*. Progression of cartilage degeneration and clinical symptoms in obese and overweight individuals is dependent on the amount of weight loss: 48-month data from the Osteoarthritis Initiative. Osteoarthritis Cartilage 2016;24(7):1126–34.
2. McDevitt C, Muir H. Biochemical changes in the cartilage of the knee in experimental and natural osteoarthritis in the dog. J Bone Joint Surg Br 1976;58(1):94–101.
3. Muir H. Heberden Oration, 1976. Molecular approach to the understanding of osteoarthrosis. Ann Rheum Dis 1977;36(3):199.
4. Mankin HJ, Thrasher A. Water content and binding in normal and osteoarthritic human cartilage. J Bone Joint Surg Am 1975;57(1):76–80.
5. Saarakkala S, Julkunen P, Kiviranta P, Mäkitalo J, Jurvelin J, Korhonen R. Depth-wise progression of osteoarthritis in human articular cartilage: investigation of composition, structure and biomechanics. Osteoarthritis Cartilage 2010;18(1):73–81.
6. Maroudas A, Venn M. Chemical composition and swelling of normal and osteoarthrotic femoral head cartilage. II. Swelling. Ann Rheum Dis 1977;36(5):399–406.
7. Mow VC, Kuei S, Lai WM, Armstrong CG. Biphasic creep and stress relaxation of articular cartilage in compression: theory and experiments. J Biomech Eng 1980;102(1):73–84.
8. Chan S, Neu C, Komvopoulos K, Reddi A. The role of lubricant entrapment at biological interfaces: reduction of friction and adhesion in articular cartilage. J Biomech 2011;44(11):2015–20.
9. Mow VC, Lai WM. Recent developments in synovial joint biomechanics. SIAM Rev 1980;22(3):275–317.
10. Chan DD, Neu CP. Probing articular cartilage damage and disease by quantitative magnetic resonance imaging. J R Soc Interface 2013;10(78):20120608.
11. Li X, Majumdar S. Quantitative MRI of articular cartilage and its clinical applications. J Magn Reson Imag 2013;38(5):991–1008.
12. Hani AFM, Kumar D, Malik AS, Ahmad RMKR, Razak R, Kiflie A. Non-invasive and in vivo assessment of osteoarthritic articular cartilage: a review on MRI investigations. Rheumatol Int 2015;35(1):1–16.
13. Blumenkrantz G, Majumdar S. Quantitative magnetic resonance imaging of articular cartilage in osteoarthritis. Eur Cell Mater 2007;13(7).
14. Ding C, Cicuttini F, Jones G. How important is MRI for detecting early osteoarthritis? Nat Clin Pract Rheumatol 2008;4(1):4–5.
15. Esmonde-White KA, Esmonde-White FW, Morris MD, Roessler BJ. Fiber-optic Raman spectroscopy of joint tissues. Analyst 2011;136(8):1675–85.
16. Rieppo L, Töyräs J, Saarakkala S. Vibrational spectroscopy of articular cartilage. Appl Spectrosc Rev 2017;52(3):249–66.
17. Unal M, Yang S, Akkus O. Molecular spectroscopic identification of the water compartments in bone. Bone 2014;67:228–36.
18. Unal M, Akkus O. Raman spectral classification of mineral- and collagen-bound water's associations to elastic and post-yield mechanical properties of cortical bone. Bone 2015;81:315–26.
19. Unal M. Classification of Bound Water and Collagen Denaturation Status of Cortical Bone by Raman Spectroscopy. Case Western Reserve University; 2017.
20. Flanagan CD, Unal M, Akkus O, Rimnac CM. Raman spectral markers of collagen denaturation and hydration in human cortical bone tissue are affected by radiation sterilization and

high cycle fatigue damage. J Mech Behav Biomed Mater 2017;75:314–21.
21. Unal M, Akkus O. Shortwave-infrared Raman spectroscopic classification of water fractions in articular cartilage ex vivo. J Biomed Optic 2018;23(1). 015008.
22. Matousek P, Stone N. Development of deep subsurface Raman spectroscopy for medical diagnosis and disease monitoring. Chem Soc Rev 2016;45(7):1794–802.
23. Demers J-LH, Esmonde-White FW, Esmonde-White KA, Morris MD, Pogue BW. Next-generation Raman tomography instrument for non-invasive in vivo bone imaging. Biomed Opt Express 2015;6(3):793–806.
24. Neu CP, Khalafi A, Komvopoulos K, Schmid TM, Reddi AH. Mechanotransduction of bovine articular cartilage superficial zone protein by transforming growth factor β signaling. Arthritis Rheumatol 2007;56(11):3706–14.
25. Arokoski J, Hyttinen MM, Lapveteläinen T, Takács P, Kosztáczky B, Módis L, *et al*. Decreased birefringence of the superficial zone collagen network in the canine knee (stifle) articular cartilage after long distance running training, detected by quantitative polarised light microscopy. Ann Rheum Dis 1996;55(4):253–64.
26. Guilak F, Ratcliffe A, Lane N, Rosenwasser MP, Mow VC. Mechanical and biochemical changes in the superficial zone of articular cartilage in canine experimental osteoarthritis. J Orthop Res 1994;12(4):474–84.
27. Sobol E, Sviridov A, Omel'chenko A, Bagratashvili V, Kitai M, Harding SE, *et al*. Laser reshaping of cartilage. Biotechnol Genet Eng Rev 2000;17(1):553–78.
28. Kwan MK, Lai WM, Van Mow C. Fundamentals of fluid transport through cartilage in compression. Ann Biomed Eng 1984;12(6):537–58.
29. Zheng B. Summarizing the goodness of fit of generalized linear models for longitudinal data. Stat Med 2000;19(10):1265–75.
30. Nakagawa S, Schielzeth H. A general and simple method for obtaining R^2 from generalized linear mixed-effects models. Methods Ecol Evol 2013;4(2):133–42.
31. Johnson PC. Extension of Nakagawa & Schielzeth's R2GLMM to random slopes models. Methods Ecol Evol 2014;5(9):944–6.
32. Liess C, Lüsse S, Karger N, Heller M, Glüer C-C. Detection of changes in cartilage water content using MRI T2-mapping in vivo. Osteoarthritis Cartilage 2002;10(12):907–13.
33. Setton L, Mow V, Müller F, Pita J, Howell D. Mechanical properties of canine articular cartilage are significantly altered following transection of the anterior cruciate ligament. J Orthop Res 1994;12(4):451–63.
34. Froimson MI, Ratcliffe A, Gardner TR, Mow VC. Differences in patellofemoral joint cartilage material properties and their significance to the etiology of cartilage surface fibrillation. Osteoarthritis Cartilage 1997;5(6):377–86.
35. Rivers P, Rosenwasser M, Mow V, Pawluk R, Strauch R, Sugalski M, *et al*. Osteoarthritic changes in the biochemical composition of thumb carpometacarpal joint cartilage and correlation with biomechanical properties. J Hand Surg 2000;25(5):889–98.
36. Treppo S, Koepp H, Quan EC, Cole AA, Kuettner KE, Grodzinsky AJ. Comparison of biomechanical and biochemical properties of cartilage from human knee and ankle pairs. J Orthop Res 2000;18(5):739–48.
37. Sah RL, Yang AS, Chen AC, Hant JJ, Halili RB, Yoshioka M, *et al*. Physical properties of rabbit articular cartilage after transection of the anterior cruciate ligament. J Orthop Res 1997;15(2):197–203.
38. Armstrong C, Mow V. Variations in the intrinsic mechanical properties of human articular cartilage with age, degeneration, and water content. JBJS 1982;64(1):88–94.
39. Rotter N, Tobias G, Lebl M, Roy AK, Hansen MC, Vacanti CA, *et al*. Age-related changes in the composition and mechanical properties of human nasal cartilage. Arch Biochem Biophys 2002;403(1):132–40.
40. Maroudas A, Bullough P. Permeability of articular cartilage. Nature 1968;219(5160):1260–1.
41. Wells T, Davidson C, Mörgelin M, Joseph L, Bayliss MT, Dudhia J. Age-related changes in the composition, the molecular stoichiometry and the stability of proteoglycan aggregates extracted from human articular cartilage. Biochem J 2003;370(1):69–79.
42. Grushko G, Schneiderman R, Maroudas A. Some biochemical and biophysical parameters for the study of the pathogenesis of osteoarthritis: a comparison between the processes of ageing and degeneration in human hip cartilage. Connect Tissue Res 1989;19(2–4):149–76.
43. Venn M. Variation of chemical composition with age in human femoral head cartilage. Ann Rheum Dis 1978;37(2):168–74.
44. Mosher TJ, Dardzinski BJ, Smith MB. Human articular cartilage: influence of aging and early symptomatic degeneration on the spatial variation of T2—preliminary findings at 3 T. Radiology 2000;214(1):259–66.
45. Bollet AJ, Nance JL. Biochemical findings in normal and osteoarthritic articular cartilage. II. Chondroitin sulfate concentration and chain length, water, and ash content. J Clin Investig 1966;45(7):1170.
46. Mankin HJ, Dorfman H, Lippiello L, zarins A. Biochemical and metabolic abnormalities in articular cartilage from osteoarthritic human hips. J Bone Joint Surg Am 1971;53(3):523–37.
47. Padalkar M, Spencer R, Pleshko N. Near infrared spectroscopic evaluation of water in hyaline cartilage. Ann Biomed Eng 2013;41(11):2426–36.
48. Palukuru UP, Hanifi A, McGoverin CM, Devlin S, Lelkes PI, Pleshko N. Near infrared spectroscopic imaging assessment of cartilage composition: validation with mid infrared imaging spectroscopy. Anal Chim Acta 2016;926:79–87.
49. Esmonde-White K. Raman spectroscopy of soft musculoskeletal tissues. Appl Spectrosc 2014;68(11):1203–18.
50. Albro M, Bergholt M, St-Pierre J, Guitart AV, Zlotnick H, Evita E, *et al*. Raman spectroscopic imaging for quantification of depth-dependent and local heterogeneities in native and engineered cartilage. NPJ Regen Med 2018;3(1):3.